Alternative GNSS antenna calibration in terms of Bernstein-Bezier polynomials

Markus Antoni, Wolfgang Keller, Tobias Kersten, Steffen Schön

antoni@gis.uni-stuttgart.de

Abstract

The reference point of an antenna is not physical fixed, but caused by electromagnetic components and their interaction. Therefore, a calibration of the antenna is required for precise point positioning.
In the Hannover concept of calibration, the code phase and the carrier phase variations are determined from the apparent changes in the short baseline vector. The variations are modeled afterwards by spherical harmonics, which leads to an unstable problem due to improper data distribution on a hemisphere.
To increase the resolution of the model, localizing spherical Bernstein-Bezier polynomials are introduced. A continuous model is achieved by condition equations during the estimation of the coefficients of the linear combination.
The new base function model even high frequencies in the data, which is not possible by spherical harmonics due to their global support.

1. Calibration

For each GNSS antenna, the calibration consist in the definition of the antenna reference point (ARP), a mean phase center offset (PCO) – the sphere of constant offset in all directions – and the pattern of the remaining phase center variations (PCV) or group delay variations (GDV), respectively (cf. Figure 1)

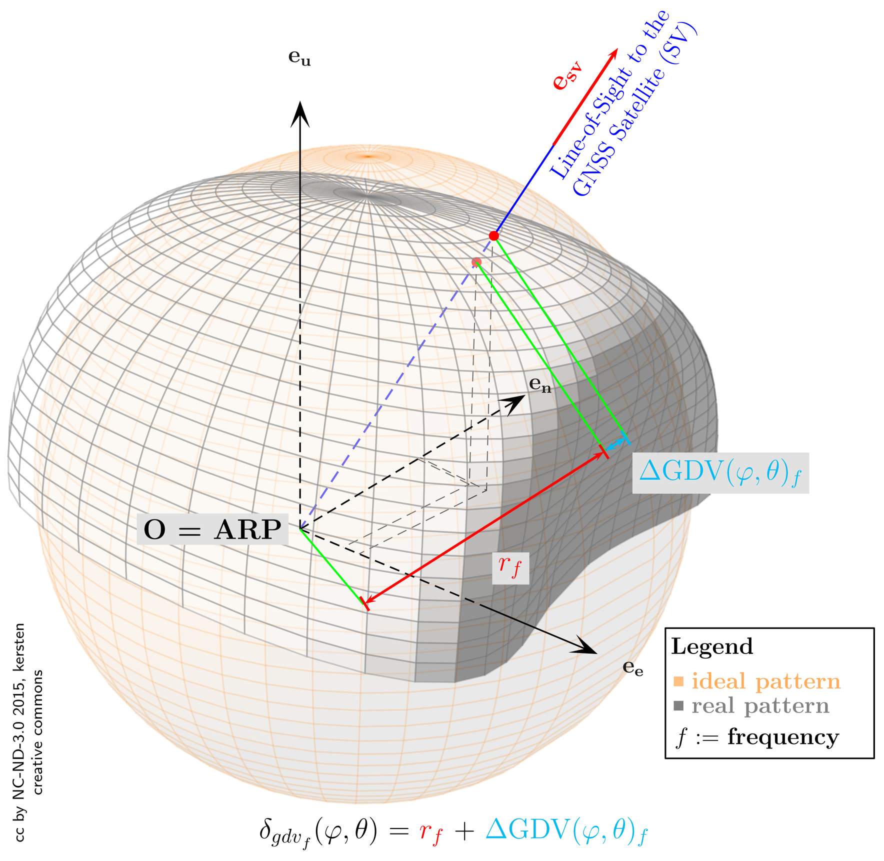

Figure 1: *Relationship between ARP, PCO and GDV*

In the Hannover concept of calibration, two antennas are set up close to each other with a common clock, and one antenna is rotated by a calibrated robot.

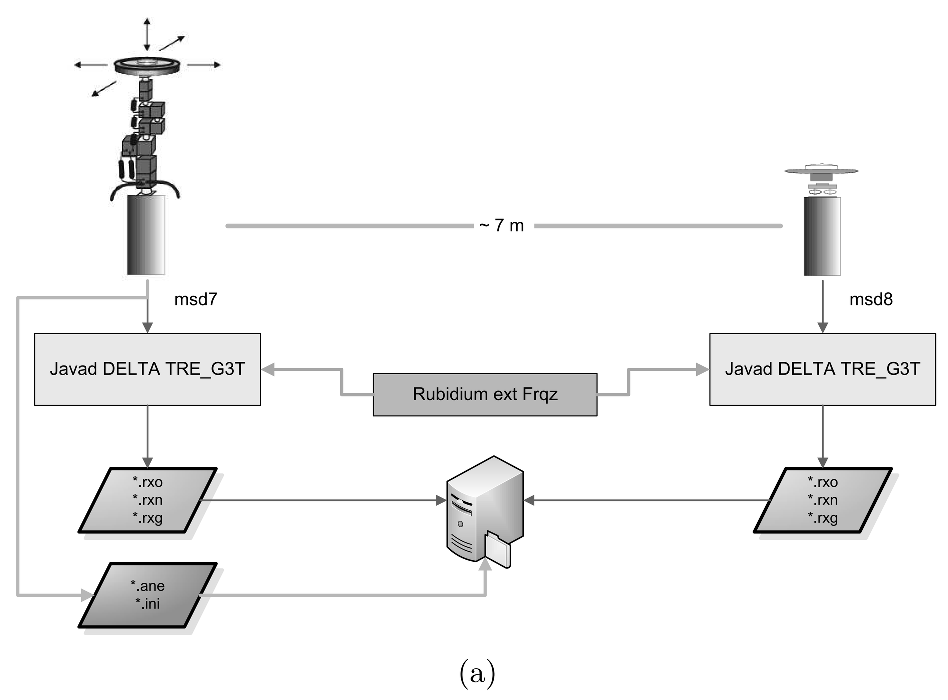

Figure 2: *Hannover concept of calibration [2]*

This setup reduces or eliminates most effects – demonstrated in the next paragraph – but disables also the separation of the PCO and clock error.

1.1 Observation model

For each frequency f, the pseudo-ranges based on code measurements between antenna A and satellite j at epoch t_ι are given by

$$P^j_{A,f}(t_\iota) = \rho_{A,f} + \delta C^j_{A,f} + \delta D^j_{A,f} + \delta S^j_{A,f}(\varphi,\theta,t_\iota) + \varepsilon_{A,f}(t_\iota)$$

with

- $\delta D_{A,f}{}^j$: delay in ionosphere and troposphere
- $\rho_{A,f}$: geometrical distance
- $\delta C_{A,f}{}^j = c \cdot t^\iota_A$: combined clock error
- $S^j_{A,f}(\varphi,\theta,t_\iota)$: phase center variations for zenith angle θ and azimuth φ in the antenna fixed frame.

Considering the reference antenna B, the single differences

$$P^j_{AB,f}(t_\iota) = P_{B,f}{}^j(t_\iota) - P_{A,f}{}^j(t_\iota) =$$
$$= \rho_{AB,f} + \delta C^j_{AB,f} + \delta D^j_{AB,f} + \delta S^j_{AB,f}(\varphi,\theta,t_\iota) + \varepsilon_{AB,f}(t_\iota)$$

are calculated.
Due to the short distance, this will remove the effects of
- ionosphere,
- troposphere and
- orbital errors.

Taking the time differences between consecutive observables $\{t_\iota, t_{\iota+1}\}$ we find the group delay variations (GDV)

$$\Delta P^j_{AB,f}(t_\iota,t_{\iota+1}) = P^j_{AB,f}(t_{\iota+1}) - P^j_{AB,f}(t_\iota) =$$
$$= \delta_{gdv_A}(\varphi,\theta) + \varepsilon_{AB,f}(t_\iota,t_{\iota+1})$$

and analogous the phase center variations (PCV) in case of phase measurements.
The multipath effects of the reference antenna B cancel out by the time differentiation, and is reduced for the test antenna by fast and calibrated rotations.

2. Modelling of the antenna pattern

2.1 Spherical harmonics

The current processing uses spherical harmonic functions – i.e. Legendre functions $\overline{P}_{nm}(\cos\theta)$ and trigonometric functions $\sin m\varphi$ and $\cos m\varphi$ – and the corresponding Stokes $\{C^{gdv}_{nm}, S^{gdv}_{nm}\}$ coefficients to model the GDVs and PCVs, respectively:

$$\begin{Bmatrix} P^j_{AB,f} \\ \Phi^j_{AB,f} \end{Bmatrix} = \sum_{n=0}^{N}\sum_{m=0}^{n}\left(\begin{Bmatrix} C^{gdv}_{nm} \\ C^{pcv}_{nm} \end{Bmatrix}\cos m\varphi + \begin{Bmatrix} S^{gdv}_{nm} \\ S^{pcv}_{nm} \end{Bmatrix}\sin m\varphi\right)\overline{P}_{nm}(\cos\theta) \qquad (1)$$

Because the spherical harmonics are orthogonal on the full sphere, but all measurements take place in the upper hemisphere of the antenna, the determination of Stokes coefficients gets unstable very fast and only low resolutions are possible. This problem could be recognized in the singular value decomposition in figure 3, where model is expanded up to maximum degree $n = 8$ and order $m = 8$. (In case of a global data set, this condition numbers corresponds to an expansion of degree 30 or 40 for optimal data distribution!)

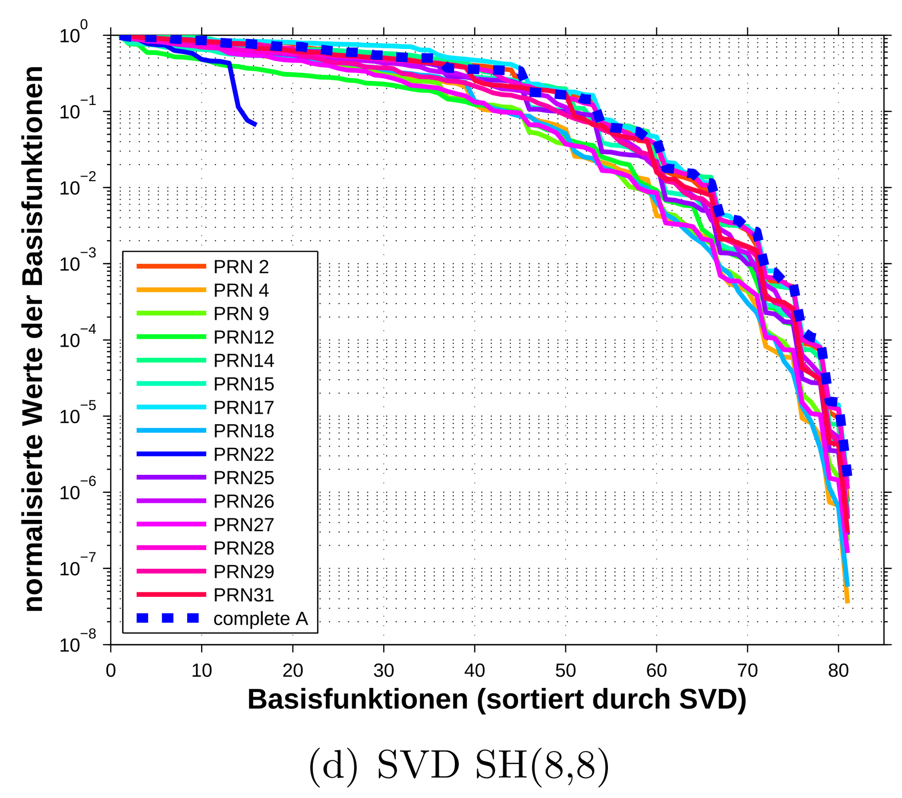

Figure 3: *Singular values per satellite for a spherical harmonic expansion up to degree and order 8 [2]*

2.2 Bernstein Bezier Splines

As an alternative, a linear combination of spherical Bernstein-Bezier polynomials (SBB) is implemented on a triangulated hemisphere. A point $\vec{x}$ inside the triangle $\Delta(\vec{p}_1,\vec{p}_2,\vec{p}_3)$ can be represented in barycentric coordinates $\Lambda_1,\Lambda_2,\Lambda_3$ with

$$\vec{x} = \Lambda_1\vec{p}_1 + \Lambda_2\vec{p}_2 + \Lambda_3\vec{p}_3. \qquad (2)$$

Each base function is defined only on a spherical triangle, and determined by harmonic polynomials [1, 3].
The antenna pattern itself is modeled by a linear combination

$$\delta_{gdv_A} = \sum_{t=1}^{T}\sum_{d=0}^{D}\sum_{i+j+k=d} c^d_{ijk}\frac{d!}{i!j!k!}\Lambda_1^i\Lambda_2^j\Lambda_3^k \qquad (3)$$

with the unknown coefficients $c^{d,t}_{ijk}$ for each triangle $1 \le t \le T$ and degree d.

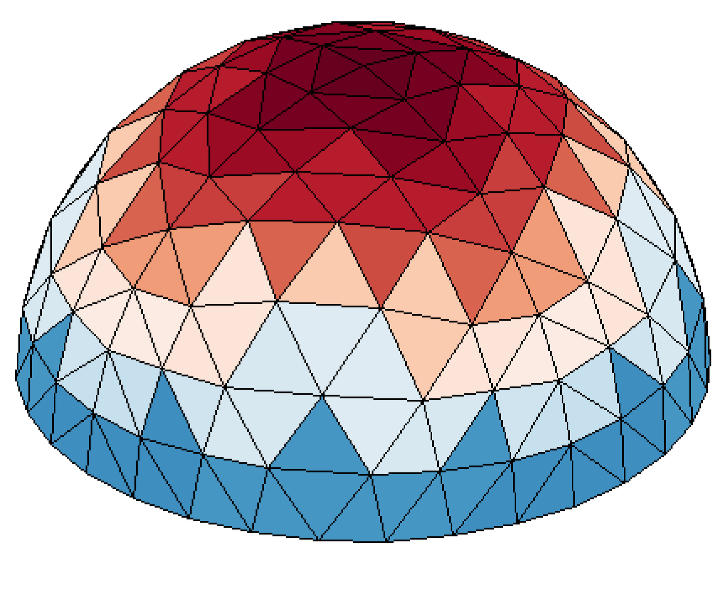

Figure 4: *triangulation of a hemi-sphere*

To ensure a continues behaviour between 2 triangles – e.g. with the corner $(\vec{p}_1,\vec{p}_2,\vec{p}_3)$ and $(\vec{p}_4,\vec{p}_2,\vec{p}_3) = (\vec{p}_{1'},\vec{p}_{2'},\vec{p}_{3'})$ the corresponding coefficients $c^{d,1}_{ijk}$ and $c^{d,2}_{ijk}$ must be equal up to reordering of the points.
Due to their local support, the functions could handle the inhomogeneous data distribution, and missing observations below the horizon will not affect the stability.

3. Comparison

In Figure 5 the observed phase center variations for a dual frequency marine antenna **ASH700700.B** are visualized for the first 14400 data points (of 28600 possible measurements) together with its approximation by spherical harmonics and Bernstein-Bezier-Splines.

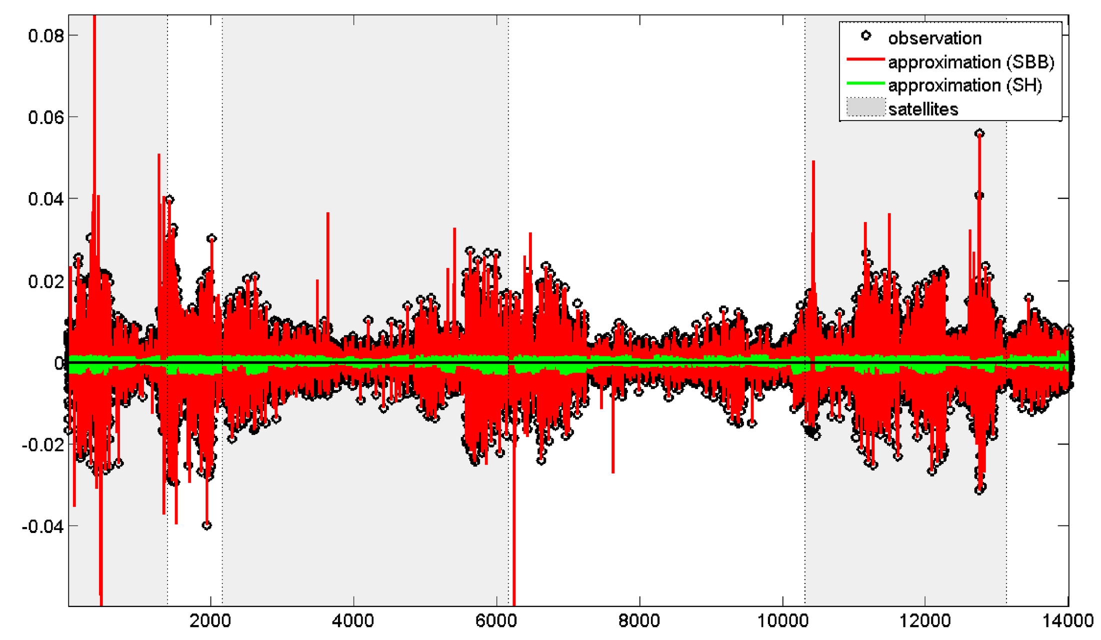

Figure 5: *Approximation of GDV by spherical harmonics and Bernstein-Bezier-Splines in $[mm]$*

- Considering the subsequent observations, the signal contains very high frequencies.
- A spherical harmonic expansion of degree and order 8 is not able to model these high frequent variations.
- The Bernstein-Bezier polynomials of degree 5 model almost all variations.
- The SBB model can partly compensate over-parametrization and stabilty problems via the smoothness- and continuity-conditions, which act as implict regularization.
- There are some outlier in the SBB modeling compared to the data. First investigations indicates problems in zenith direction, which might be caused by the triangulation algorithm in combination with the over parametrization.

References

[1] P. Alfeld, M. Neamtu, L. L. Schumaker: *Bernstein-Bezier polynomials on spheres and sphere-like surfaces* Computer Aided Geometric Design 13, pp. 333-349, 1996

[2] T. Kersten: *Bestimmung von Codephasen-Variationen bei GNSS-Empfangsantennen und deren Einfluss auf die Positionierung, Navigation und Zeitbertragung* PhD thesis, 315, Leibniz Universität, Hannover, 2014

[3] M. J. Lai, C. K. Shum, V. Baramidze, P. Wenston *Triangulated spherical splines for geopotential reconstruction* J. Geod., Springer, 2008

University of Stuttgart
Germany